Entanglement transitions in random pure states

Hassan Shapourian[1] and Jonah Kudler-flam[2]

[1] *Microsoft Station Q, Santa Barbara, CA 93106, USA*

[2] *Kadanoff Center for Theoretical Physics, University of Chicago, IL 60637, USA*

(Dated: September 18, 2020)

In this paper, we use large-N perturbation theory to compute the entanglement negativity of random induced mixed states. Our result reproduces the two well-known limits: volume law states and separable states. We also find that the volume law states can be further divided into two categories in terms of subsystem-size scaling of the entanglement negativity: a linear scaling phase, where the state is maximally entangled and the logarithmic negativity is bound by the size of the smaller subsystem $\mathcal{E} \sim V_{A_1}$, and a saturated phase, where $\mathcal{E} \sim (V_A - V_B)/2$, which is independent of individual subsystem sizes V_{A_1} and V_{A_2}. In the latter case, the spectral density can be well-approximated by a semi-circle law. We show that the large-N perturbation theory results match with those of the random matrix simulations. Our finding indicates that the average logarithmic negativity behaves very similar to the 1/2-Rényi mutual information.

I. INTRODUCTION

Random pure states represent typical volume law entangled (thermal) pure states. Their virtue is that they are described by Wishart random matrix theory and hence, various well-established random matrix theory tools are available to carry out calculations on them.

In this paper, we use the large-N perturbation theory which was recently developed by one of us [1] to compute the spectral density of partial transpose and characterize the reduced density matrix in several limits. The result is summarized in Fig. 1.

We would like to study the entanglement in random mixed states obtained by partial tracing over random pure states. Concretely, consider a random pure state, aka Page state (or Haar state), $|\Psi\rangle$ in a composite Hilbert space $\mathcal{H} = \mathcal{H}_A \otimes \mathcal{H}_B$. Here, the word random means uniformly distributed on the sphere of the Hilbert space $\mathcal{H}$. An ensemble of reduced density matrices $\{\rho\}$ acting on the Hilbert space $\mathcal{H}_A = \mathcal{H}_{A_1} \otimes \mathcal{H}_{A_2}$ is generated by $\rho_A = \mathrm{Tr}\,|\Psi\rangle\langle\Psi|$. It is more convenient to represent such a random pure state in a tensor product basis as in

$$|\Psi\rangle = \sum_{i=1}^{L_A} \sum_{\alpha=1}^{L_B} X_{i\alpha}\, |\Psi_A^{(i)}\rangle \otimes |\Psi_B^{(\alpha)}\rangle, \tag{1}$$

in terms of a $L_A \times L_B$ rectangular random matrix X whose elements $(X_{i\alpha})$ are independent random complex variables. Here, $L_A = L_{A_1} \times L_{A_2}$ and L_B denote the size of $\mathcal{H}_A$ and $\mathcal{H}_B$, respectively. Throughout this paper, we consider A and B systems to be comprised of qubits. In other words, $L_s = 2^{V_s}$ where $s = A_1, A_2, B$ and V_s is the number of qubits. This choice is not a necessary ingredient for our calculations and is mainly meant as a physical description of the system.

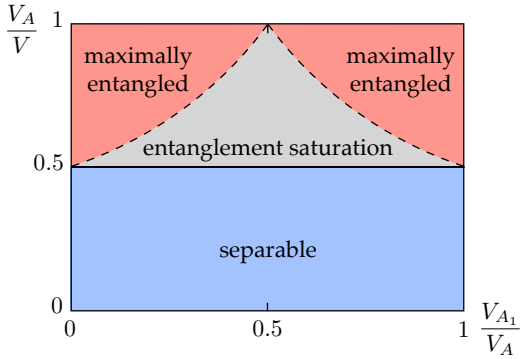

FIG. 1. Phase diagram of reduced density matrix obtained from random pure states (or Page states).

By definition, the joint probability density is given by

$$P\left(\{X_{i\alpha}\}\right) = \mathcal{Z}^{-1} \exp\left\{-L_A L_B \mathrm{Tr}(XX^\dagger)\right\}. \tag{2}$$

The random reduced density matrix of system A is then given by

$$\rho_A = \frac{XX^\dagger}{\mathrm{Tr}(XX^\dagger)}. \tag{3}$$

We note that ρ_A is a $L_A \times L_A$ square matrix, and the denominator (which is also a random variable) is there to enforce the normalization condition $\mathrm{Tr}\rho_A = 1$.

The eigenvalues of ρ_A (aka the entanglement spectrum) contains information about the entanglement between A and B. In the limit $L_A, L_B \to \infty$ while the ratio L_A/L_B is finite (which we will refer to as the large L limit from now on), the joint probability density function of these eigenvalues can be derived [2, 3]. In doing so, the crucial approximation is that the normalization factor in Eq. (3) is a random variable $\mathrm{Tr}(XX^\dagger) = 1 + \delta$ whose fluctuations about its mean 1 is negligible to the leading order in $L_A L_B$. Hence, to the leading order, the denominator can be approximated by its mean value, and we may write

$$\rho_A \approx XX^\dagger. \tag{4}$$

which is the celebrated Wishart-Laguerre ensemble [4] and is extensively studied in the random matrix theory literature. From this observation, one can infer several properties of ρ_A in the large L limit. Among all, the spectral density of the eigenvalues is given by an appropriately scaled Marcenko-Pastur (MP) function [4]. In the following sections, we present a graphical representation for ρ_A and its partial transpose $\rho_A^{T_2}$ which will be used to calculate the spectral density of eigenvalues of ρ^{T_2}.

II. LARGE-N PERTURBATION THEORY

In this section, we use graphical representation of a partially transposed random mixed state to compute its momets and eventually derive the corresponding resolvent function and the spectral density.

We begin by reviewing the diagrammatic approach to random pure states [5, 6]. This method is based on the 't Hooft $1/N$ (double line) perturbation theory which was also used recently in the context of black hole information problems [7].

A matrix element of the pure state density matrix (1) is denoted as

$$\left[|\Psi\rangle\langle\Psi|\right]_{i\alpha,j\beta} = X^*_{i\alpha}X_{j\beta} =$$

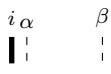

, (5)

where the left (right) pair of lines represents a bra (ket) state, and solid (dashed) lines correspond to subsystem A (B). Note that each line carries an index. The lower end of the diagrams are reserved for matrix manipulations such as tracing and multiplication, while the upper ends of the lines are used for ensemble averaging. Hence, a matrix element of the reduced density matrix is represented by

$$[\rho_A]_{i,j} = \sum_{\alpha=1}^{L_B} X^*_{i\alpha}X_{j\alpha} =$$

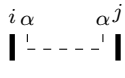

. (6)

For brevity, from now on we drop the subscript A in ρ_A unless stated otherwise. Moreover, ensemble averaging is achieved by connecting the upper terminals by

$$\langle X_{i\alpha}H_{j\beta}\rangle \equiv$$

$$= \frac{1}{L_A L_B}\,\delta_{i_1 j_1}\delta_{i_2 j_2}\delta_{\alpha\beta}. \tag{7}$$

For instance, the normalization condition on average is represented by the diagram, For example, we may write

$$\langle \mathrm{Tr}\rho\rangle =$$

$$= 1. \tag{8}$$

We now incorporate the partial transpose as an operation on the density matrix (6). First, we note that we need a tri-partite geometry; in other words, subsystem A is further partitioned into A_1 and A_2. So, we define a (more refined) bipartite reduced density matrix by

$$[\rho]_{i_1 i_2, j_1 j_2} = \sum_{\alpha} X^*_{(i_1 i_2),\alpha} X_{(j_1 j_2),\alpha} = \quad , \tag{9}$$

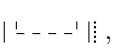

where the dotted and solid lines correspond to subsystems A_1 and A_2, respectively. Partial transpose is diagrammatically shown as

$$[\rho^{T_2}]_{i_1 i_2, j_1 j_2} = \sum_{\alpha} X^*_{(i_1 j_2),\alpha} X_{(j_1 i_2),\alpha} = \quad . \tag{10}$$

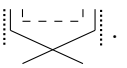

The underlying operation in the above diagram is to swap the indices for one subsystem as emphasized by indices highlighted in red. Such implementation of the partial transpose is indeed not limited to random density matrices and can be applied to deterministic density matrices of spin chains. In the latter context, we need to impose certain rules on the diagrammatic representation of the partial transpose to make it consistent with time-reversal symmetry. For instance, Penrose diagrams [8, 9] provides such a consistent representation which can be used to derive the Z_2 topological invariant for topological phases of spin chains protected by time-reversal symmetry [10].

One can easily check that the above definition of partial transpose is trace preserving and does not change the purity, i.e. $\mathrm{Tr}{\rho^{T_2}}^2 = \mathrm{Tr}\rho^2$.

A. Moments of partial transpose

Let us look at the dominant diagrams deep in the NPT limit, $L_A \gg L_B$, when one subsystem (A_1 or A_2) is much larger than the other.

$$\langle \mathrm{Tr}\left(\rho^{T_2}\right)^{n_e} \rangle \approx \begin{cases} L_B^{1-n_e} L_{A_2}^{2-n_e} & L_{A_1} \gg L_{A_2} \\ L_B^{1-n_e} L_{A_1}^{2-n_e} & L_{A_1} \ll L_{A_2} \end{cases} \tag{11}$$

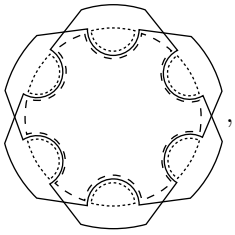

, (12)

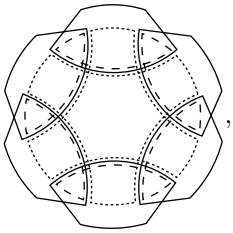

, (13)

TMD spacetime conjecture vs RMT (assuming $L_{A_1} \gg L_{A_2}$):

$$\langle \mathrm{Tr}\left(\rho^{T_2}\right)^{n} \rangle \approx \begin{cases} \text{genus } k-1 \text{ with } 1\times\text{puncture} & n\times A_1, 1\times A_2, 1\times B & n = 2k+1 \\ \text{genus } k \text{ with } 2\times\text{punctures} & n\times A_1, 2\times A_2, 1\times B & n = 2k \end{cases} \tag{14}$$

This suggests that

$$\langle \mathcal{E} \rangle \approx \begin{cases} \log L_{A_2} & L_{A_1} \gg L_{A_2}, \\ \log L_{A_1} & L_{A_1} \ll L_{A_2}. \end{cases} \tag{15}$$

This analysis may have some issues such as dependence on how we analytically continue Rényi index. In the next part, we use the resolvent function to calculate the spectral density of ρ^{T_2} which provides an unambiguos way to derive the logarithmic negativity.

B. Resolvent function

Our goal in this part is to derive the spectral density of the partially transposed density matrix. To this end, we define a one-point Green function (or a resolvent function) as

$$G(z) = \frac{1}{L_A} \left\langle \mathrm{Tr}\left(\frac{1}{z-H}\right)\right\rangle, \tag{16}$$

where we use a particular normalization and define $H = L_B L_{A_2} (XX^\dagger)^{T_2}$ to carry out calculations systematically such that $1/N$ perturbative expansion makes sense. The actual normalization will be included via rescaling after the spectral density is evaluated. We can then compute the spectral density using the identity

$$P_\Gamma(\xi) = -\frac{L_A}{\pi} \mathrm{Im} \lim_{\epsilon\to 0} G(z)\big|_{z=\xi+i\epsilon}, \tag{17}$$

because

$$\lim_{\epsilon\to 0} \frac{1}{\lambda + i\epsilon} = \mathrm{PV}\,\frac{1}{\lambda} - i\pi\delta(\lambda). \tag{18}$$

The Feynman diagram approach follows by expanding $G(z)$ in inverse powers of z. In our graphical representation of a given term, we insert the diagram (10) for every power of ρ^{T_2}. The ensemble average is represented by triple lines with amplitude $1/L_{A_1}$ (given the above normalization),

$$\langle H_{i_1 j_1 \alpha} H_{i_2 j_2 \beta}\rangle \equiv \quad = \frac{1}{L_{A_1}} \delta_{i_1 j_1}\delta_{i_2 j_2}\delta_{\alpha\beta}, \tag{19}$$

and as usual close loop of subsystem $s = A_1, A_2$, or B gives a factor of L_s.

We note that since there is an even/odd effect for the Rényi negativity, we need to consider two self-energy functions in the expansion of the resolvent function

$$\begin{aligned} G &= + \Sigma_o + \Sigma_e \\ &\quad + \Sigma_o \Sigma_e + \Sigma_e \Sigma_o + \cdots \\ &= \frac{1}{z - \Sigma_o(z) - \Sigma_e(z)}, \end{aligned} \tag{20}$$

where

$$\Sigma_o = \quad + \quad + \cdots, \tag{21}$$

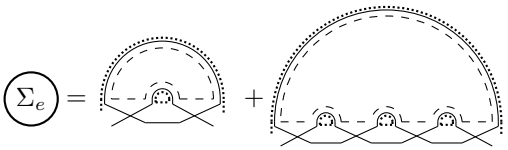

(22)

corresponding to effectively crossing and non-crossing diagrams of order L_B/L_{A_1} and $L_B L_{A_2}/L_{A_1}$, respectively. To derive a Schwinger-Dyson equation we first define

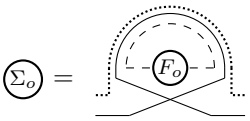

(23)

and

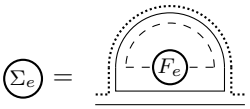

(24)

which lead to the following algebraic relations,

$$\Sigma_o(z) = \alpha F_o(z), \tag{25}$$
$$\Sigma_e(z) = \beta F_e(z), \tag{26}$$

Here, the Hilbert space dimension ratios are given by

$$\alpha = \frac{L_B}{L_{A_1}}, \qquad \beta = \frac{L_B L_{A_2}}{L_{A_1}}. \tag{27}$$

Next, we write self-consistent conditions for F-functions as in

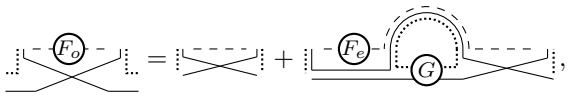

(28)

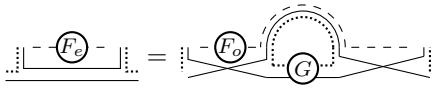

(29)

which lead to the following algebraic relations

$$F_o(z) = 1 + F_e(z)G(z), \tag{30}$$
$$F_e(z) = F_o(z)G(z). \tag{31}$$

They can be solved in terms of $G(z)$ as in

$$F_2(z) = G(z) \cdot F_1(z) = \frac{G(z)}{1 - G^2(z)}. \tag{32}$$

Solving the self-energy equation for $G(z)$, we obtain the following cubic equation

$$zG^3(z) + (\beta - 1)G^2(z) + (\alpha - z)G(z) + 1 = 0. \tag{33}$$

The proper solution to the above equation can be written as

$$G(z) = \frac{e^{-i\theta}Q(z)}{(R(z) + \sqrt{D(z)})^{1/3}} - e^{i\theta}(R(z) + \sqrt{D(z)})^{1/3} + \frac{1 - \beta}{3} \tag{34}$$

where $\theta = \pi/3$.

$$Q(z) = \frac{3z(\alpha - z) + (\beta - 1)^2}{9z^2}, \tag{35}$$

$$R(z) = \frac{9z(\beta - 1)(\alpha - z) - 27z^2 - 2(\beta - 1)^3}{54z^3}, \tag{36}$$

$$D(z) = Q^3(z) + R^2(z). \tag{37}$$

In the limit, $L_{A_1} \ll L_B L_{A_2}$, we have $\beta \gg 1$. Upon appropriate rescaling of variable $z \to y L_{A_2}$ which also implies $G(z) \to L_{A_2}^{-1} \tilde{G}(y)$ where $\tilde{G}(y) := G(y L_{A_2})$, we obtain

$$\frac{y}{L_{A_2}^2} \tilde{G}^3(y) + (r - \frac{1}{L_{A_2}^2}) \tilde{G}^2(y) + (r - y)\tilde{G}(y) + 1 = 0, \tag{38}$$

in which $r = L_B/L_A$. The $1/L_{A_2}$ terms are negligible and we arrive at

$$r\tilde{G}^2(y) + (r - y)\tilde{G}(y) + 1 = 0. \tag{39}$$

that is the semi-circle law.

III. CONCLUSIONS

Discussion on properties of spectral density at critical points At the critical point, we have $\beta = 1$,

$$zG^3(z) + (\alpha - z)G(z) + 1 = 0. \tag{40}$$

spectral density diverges as $1/z^{1/2}$ near $z = 0$ similar to the Page transition...

ACKNOWLEDGMENTS

[1] H. Shapourian, S. Liu, and A. Vishwanath, to appear (2020).
[2] S. Lloyd and H. Pagels, Annals of Physics **188**, 186 (1988).
[3] K. Zyczkowski and H.-J. Sommers, Journal of Physics A: Mathematical and General **34**, 7111 (2001).
[4] P. Forrester, *Log-Gases and Random Matrices* (Princeton University Press, Princeton, NJ, 2010).
[5] J. Jurkiewicz, G. Lukaszewski, and M. Nowak, Acta Phys. Pol. B **39**, 799 (2008).
[6] E. Brézin and A. Zee, Nuclear Physics B **453**, 531 (1995).
[7] G. Penington, S. H. Shenker, D. Stanford, and Z. Yang, arXiv:1911.11977 (2019).
[8] R. de Pietri and C. Rovelli, Phys. Rev. D **54**, 2664 (1996), gr-qc/9602023.
[9] C. Rovelli, *Quantum gravity*, Cambridge Monographs on Mathematical Physics (Cambridge Univ. Pr., Cambridge, UK, 2004).
[10] H. Shapourian, R. Mong, and S. Ryu, to appear (2020).